Accepted Manuscript

Friction welding for the manufacturing of PA6 and ABS structures reinforced with Fe particles

Ranvijay Kumar, Rupinder Singh, I.P.S. Ahuja, Ada Amendola, Rosa Penna

PII: S1359-8368(17)32237-0

DOI: 10.1016/j.compositesb.2017.08.018

Reference: JCOMB 5243

To appear in: *Composites Part B*

Received Date: 30 June 2017

Revised Date: 29 August 2017

Accepted Date: 29 August 2017

Please cite this article as: Kumar R, Singh R, Ahuja IPS, Amendola A, Penna R, Friction welding for the manufacturing of PA6 and ABS structures reinforced with Fe particles, *Composites Part B* (2017), doi: 10.1016/j.compositesb.2017.08.018.

Friction welding for the manufacturing of PA6 and ABS structures reinforced with Fe particles

[1,2]Ranvijay Kumar [1]Rupinder Singh*, [2]IPS Ahuja, Ada Amendola[3] and Rosa Penna[3]
[1]Dept. of Production Engineering, Guru Nanak Dev Engineering College, Ludhiana (India)
[2]Dept. of Mech. Engineering, Punjabi University, Patiala (India)
[3]University of Salerno, Italy
[1,2]ranvijayk12@gmail.com [1]rupindersingh78@yahoo.com, [2]ahujaips@gmail.com, [3*]adamendola@gmail.com, [3]rpenna@unisa.it
*Corresponding author

Abstract: In the present work PA6 matrix reinforced with metal powder (Fe) has been joined by friction welding with ABS matrix reinforced with Fe powder for structural applications (like: joining of pavement sheets, assembly of pipe lines etc.). The melt flow index (MFI) of PA6+Fe powder was put approximately equivalent to MFI of ABS + Fe powder by varying the proportion of Fe powder in PA6 and ABS matrix. After fixing proportion of Fe powder in PA6 and ABS material, these materials were used for preparation of feed stock filament of fused deposition modelling filament (FDM) by screw extrusion process. Finally two FDM filaments of PA6+Fe powder and ABS+Fe powder were fed into FDM machine independently. The functional prototypes of circular cross-section were prepared on FDM machine (one with filament of PA6+ Fe powder and second with ABS+Fe powder). These geometrical shapes of two dissimilar plastic/polymer materials were used on friction welding setup. Finally under best parametric conditions of feed, rpm etc. these reinforced polymer materials were successfully joined. This study provides a response surface methodology (RSM) based statistical model for enhancing the weldability of dissimilar polymer materials (as an alternative method) with improved mechanical/ metallurgical properties.

Keywords Polymer welding, Friction welding, ABS, Nylon6, dissimilar thermoplastics, MFI

Abbreviations

ABS: Acrylonitrile butadiene styrene

DSC: Differential scanning calorimeter

MFI: Melt flow index

PA6: Polyamide 6

RSM: Response surface methodology

1 Introduction

Friction welding is also known as solid state process that joins similar and dissimilar metallic or polymeric based materials. This is considered originally a conventional forming process that has a history as far back as the “Bronze age”, when gold coins and complex structures were formed through application of pressure welding. One of the great evidence of this technique can be seen as “Iron pillar” at Delhi India, which was made around 1700 year ago. The friction welding as

professional techniques has emerged in the beginning of 20th century [1]. Along with friction welding, there are other solid state welding techniques capable for joining of dissimilar plastic based material. One of the solid state welding processes, known as ultrasonic welding which is best applicable as “ease of automation” among all its kind [2]. But this process cannot be considered as economical process for field application as compared to the friction welding. Microwave welding is assumed to be the best applicable technique for joining of inherently conducting polymers [3], but most of the polymers are considered as non-conducting in nature so application of microwave welding is very limited. The researchers in the field of solid state welding of amorphous polymers have introduced a term called “healing” which has been explained as when two same amorphous polymers contacted to each other at temperature greater than their glass transition temperature, resulted into formation of bond layer, it is known as healing [4]. The another process named CO_2 laser welding emerged as a newer solid state welding technique which has the capability to weld the non-conducting polymers [5], but this laser welding concept is not a cost effective process anymore. The variety of finite element modeling and numerical modeling for solid state welding of polymer welding has been developed by the researchers. A dynamic Monte-Carlo lattice model has been developed for simulation of polymer chain at welded face undergone to welding process [6]. The amorphous thermoplastic like: polyetherimide (PEI), which natured as high melting point polymer can be joined with hot tool welding [7]. Similar to dynamic Monte Carlo lattice model, another simulation model has been developed by the researcher called “Meso scale model” for welding of polymers [8]. The another solid state welding variant known as vibration welding, is used for joining of complex structure parts fabricated from injection molding [9]. Under the categories of solid state welding processes, the resistance welding has emerged as a solid state welding process that has great potential for high performance application of fiber reinforced thermoplastic composites welding [10]. The reinforcement of metallic or nonmetallic fillers like Fe, Al, Cu, glass fiber, carbon fiber always lead to contribution of better mechanical or metallurgical properties. The researchers have observed the formation of a hybrid layer in between the welded interface which contributed to the better mechanical properties, by resistance welding of carbon fiber reinforced PEI [11]. Other than thermoplastic materials, electrical resistance welding can be best applicable for the welding of thermo-set materials [12]. Unlike fusion bonding, auto-adhesion is a variant of solid state welding technique that is used for the welding/joining of polymeric materials [13]. Friction welding technique was originally come into existence for joining similar metallic pieces only [14].But later on much research has been carried towards feasibility of friction welding for dissimilar metals like; steel-aluminum and steel-copper and aluminum-magnesium cylindrical piece joining [15-16]. The researcher in present era aims for welding of dissimilar polymers. Some studies have been reported the mechanism of friction welding for dissimilar polymeric material like; ABS and high density polyethylene (HDPE) [17]. The investigations for mechanical, thermal, and metallurgical properties for frictionally welded joints have been made [18-20]. Fusion, bonding, deformation and microstructure at welded interface have been investigated by the scanning electron

microscope (SEM) to check the effects of input process [16, 21-22].The study outlined that joining of similar polymer (ABS/Nylon6 etc.) to itself is very much feasible. Along with this joining of dissimilar polymers (like ABS to HDPE) is also feasible. The effect of using threaded pin for friction stir welding of Nylon6 plates has improved mechanical mixing at the joint interface [23].The researcher have developed different techniques of solid state welding and its variant. But there is a limitation of joint strength (for friction welded joints) of these thermoplastics that hinders its use in different engineering applications. Friction welding has emerged as repair and maintenance tool, where two oil or gas pipeline can be joined together by using a friction welding variant called "Friex" [24]. Friction inertia welding concept is widely accepted in aerospace applications [25]-[26]. Reinforcement of nano-composite or metal powder in thermoplastic matric leads to better joining efficiency with friction welding. The studies have been conducted to check the improvement in joint strength with use of SiO_2 nano-composite in welding of poly (methylmethacrylate) PMMA. The welding of PMMA-SiO_2 was observed to be possible with better mechanical strength [27]. It has been established that the reinforcement of nano-composite (carbon nanotube, grapheme and nano sized metal powder) with polymers is responsible for the improved mechanical and metallurgical properties [28-32].

The literature review reveals that lot of work has been reported for friction welding of metals, non-metals or thermoplastic for different areas of applications [33-39]. But hitherto, very less has been reported for friction welding of dissimilar polymers like; PA6 and ABS. This work is an extension of work performed by Singh et al. [39] (especially as regards to thermal characterization and statistical modelling). In the present work attempts have been made to perform friction welding for FDM printed dissimilar thermoplastic (ABS and PA6) by reinforcement of Fe metals powder with preview of rheology and compatibility in terms of thermal and mechanical properties.

2 Experimental

2.1 Materials

PA6 is an engineering thermoplastic material that has extensive application in different areas like; automobile, construction and repairs (Civil engineering), aerospace and used as rapid tooling in medical field. PA6 has good material characteristics like; wear or erosion resistivity, thermal, chemical and dimensional stability, excellent elongation properties and etc. Acrylonitrile linked to long carbon chain of ABS contributes as high strength, whereas butadiene and styrene enhance the molding and additive manufacturing capability. ABS has good impact and toughness properties. ABS is amorphous in nature and has no true melting point but has a melting range. Table 1 shows the relative comparison of ABS and PA6 based upon different mechanical, thermal and chemical properties.

Table1 Mechanical, chemical and thermal properties of ABS and PA6 [33-37]

Properties	ABS	PA6
Tensile strength (kgf/mm^2)	3.516-5.274	4.219-16.878
Flexural strength (kgf/mm^2)	189.881-267.240	274.272-773.590
Chemical resistance	Poor to fair	Good to excellent
Glass transition temperature (^oC)	105	46
Melting point (^oC)	No true melting(amorphous)	215^oC
Chemical formula	$(C_8H_8 \cdot C_4H_6 \cdot C_3H_3N)_n$	$(C_6H_{11}NO)_n$
Density (g/cm^3)	0.9–1.53	1.084
Specific heat capacity (J/kg.K)	1300	1600

2.2 MFI analysis

MFI is a consideration of material characteristics and it determines the rheological behavior of polymers [40]. Various studies have been contributed to establish the relationship between MFI, mechanical and thermal properties [41-46]. Most of the polymers are investigated for their MFI (g/10min) as per ASTM D1238 standard (at temperature of 230^oC and applied mass of 3.8Kg). Fig. 1 shows the experimental setup for MFI investigation. Table 2 shows the MFI of ABS and PA6 with different proportion of Fe powder concentration.

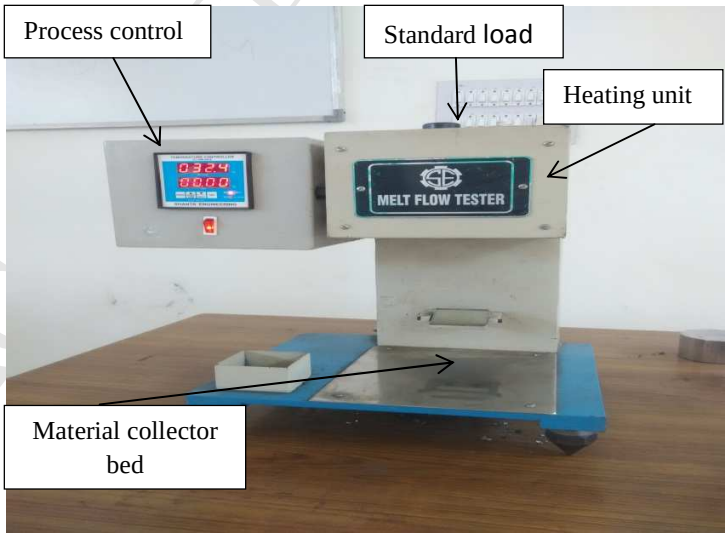

Fig. 1 MFI setup

Table 2 MFI of ABS and PA6 with different proportion of Fe powder concentration

Wt. % of Fe	MFI with ABS	MFI with PA6
0	8.898	9.972
10	10.344	11.249
20	11.973	12.615
30	13.681	14.208
40	15.075	15.006
50	16.141	16.786

As it was observed from Table2, MFI for ABS and PA6 material is almost in similar range at 40% Fe concentration. So based upon MFI results, 40% Fe proportion in ABS/PA6 has been selected for further experimentations. Based upon Table 2, Fig. 2 shows graphical representation of MFI investigation of ABS and PA6 with different proportion of Fe. It has been observed that with increase in Fe powder in polymer matrix, MFI also increases.

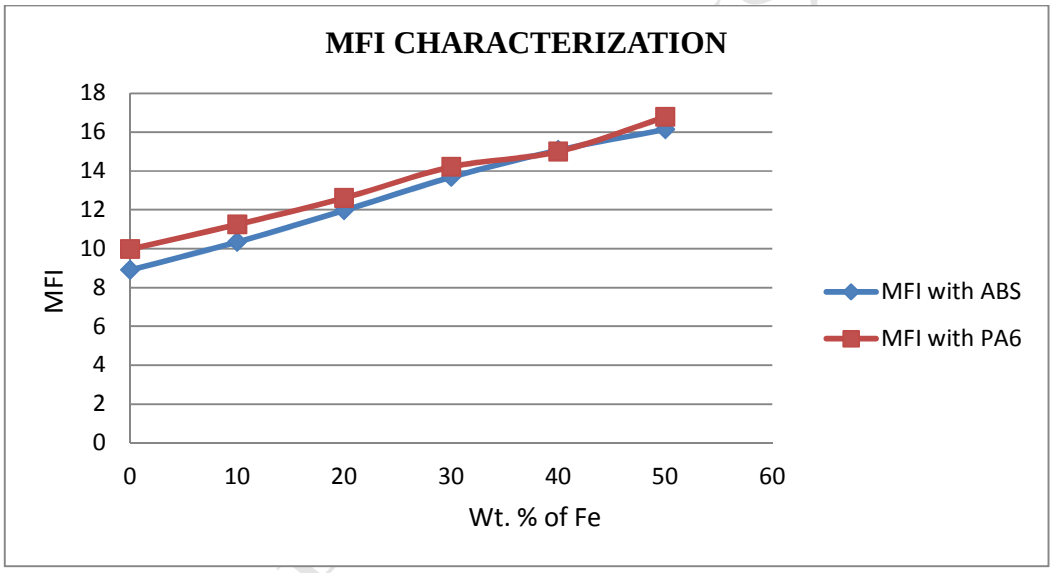

Fig. 2 Variation of MFI relative to concentration of Fe metal powder

2.3 DCS analysis

DSC is an experimental setup that analyses melting behavior, solidification characteristic and glass transition temperature etc. In this study, DSC evaluation was performed under controlled experimental environment conditions of continuous heating (endothermic changes, 10^{o}C/min) and continuous cooling (exothermic changes, 10^{o}C/min) in 30-250^{o}C temperature range.Thermal properties were analyzed bytwo continuous endothermic and exothermiccycles at 50ml/min of N_2 gas supply. The typical DSC setup determines the behavior of applied samples by taking references from standard sample, both enclosed in a metallic crucible (Al or platinum). Fig. 3 shows DSC setup which uses two separate crucibles for heating and cooling, (one for reference

and another for sample to be investigated). Fig. 4 shows the graphical representation for comparison of natural ABS and ABS-40%Fe.

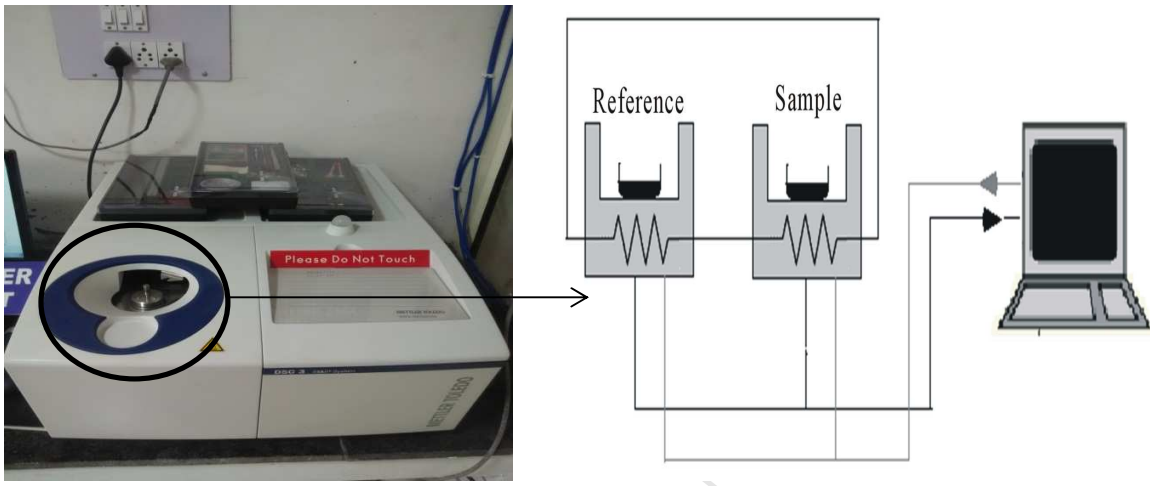

(a) (b)

Fig. 3(a) DSC setup and (b) heat inflow chamber for sample

As observed from Fig. 4, ABS-40%Fe has greater melting point as compared to natural ABS whereas specific heat capacity has reduced as compared to natural ABS. This may be due to the presence of Fe metal powder. So, it has been ascertained that Fe metal powder contributes to the change (increase) in melting point for ABS polymer matrix.

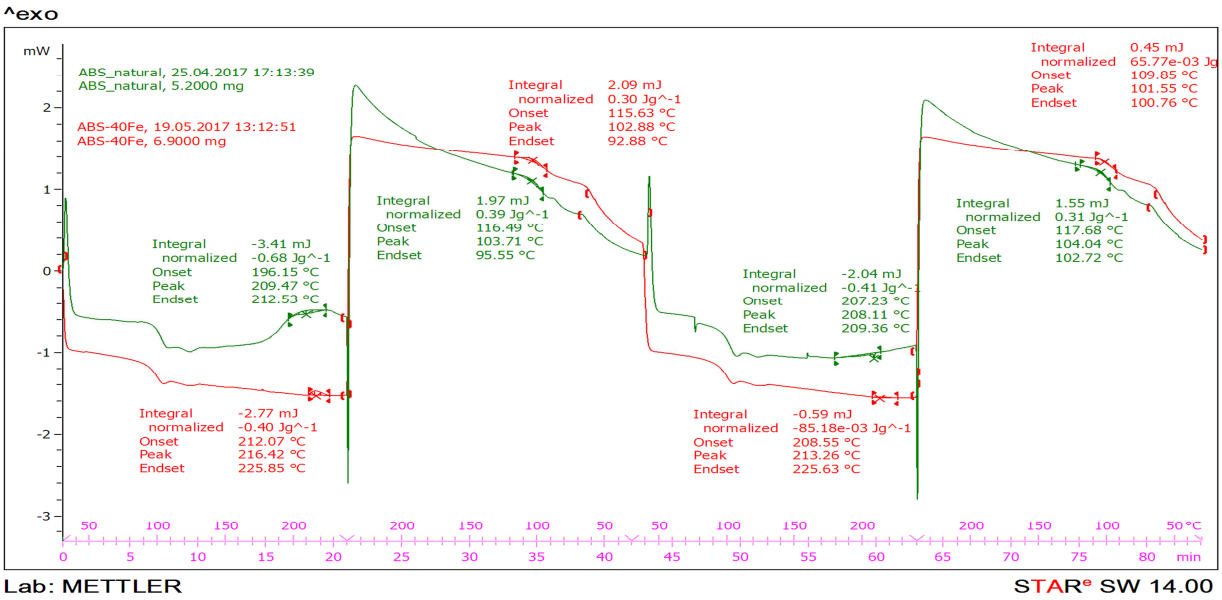

Fig. 4 DSC comparison for natural ABS and ABS-40%Fe

In the case of PA6 polymer matrix, 40% Fe metal powder proportion lowered the melting in small range (see Fig. 5).

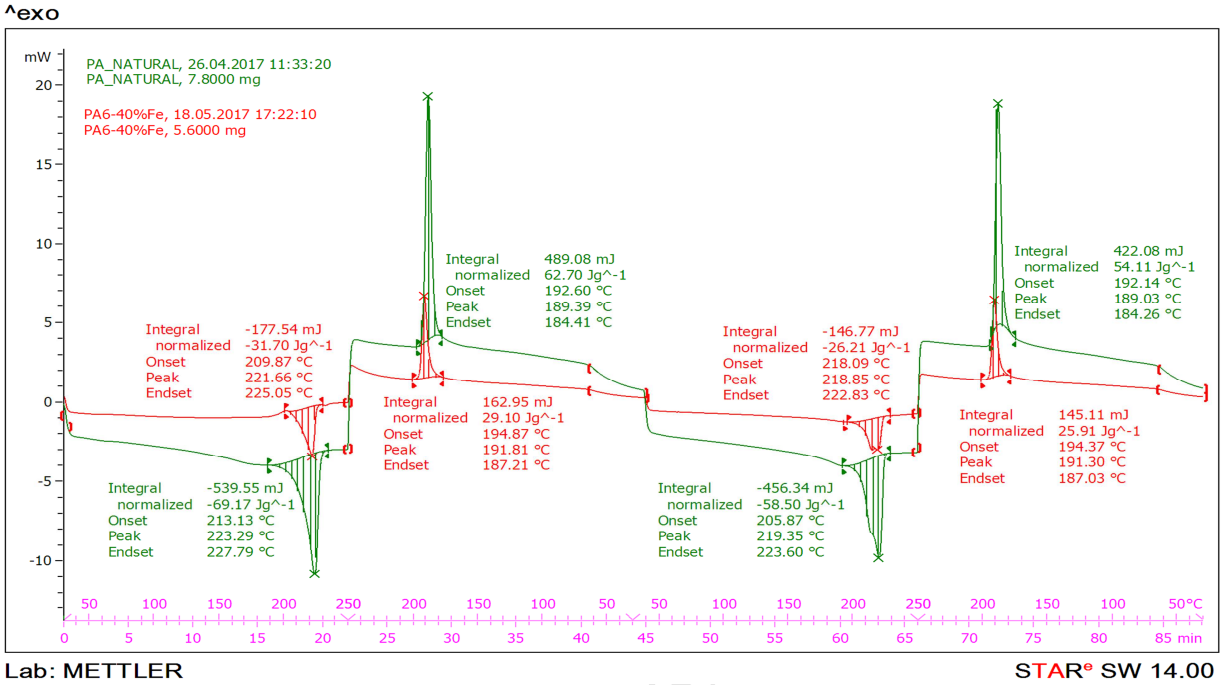

Fig. 5 DSC comparison for PA6 and PA6-40%Fe

As observed from Fig. 4, in the case of ABS polymer matrix, initially melting range of natural ABS was observed in the range of 196.15-212.53^{o}C, but ABS with 40% Fe was in between 212.07-225.85^{o}C. The natural PA6 was observed for melting temperature range in between 213.13-227.79^{o}C which was little higher than PA6-40%Fe in the range of 209.87-225.05^{o}C (See Fig. 5). It was observed that at 40% Fe metal powder concentration both polymer matrix came into a similar melting range.

2.4 Twin screw extrusion

Twin screw extruder setup was used to prepare feedstock filament for FDM setup (See Fig. 6)

Fig. 6 Twin screw extruder

The feedstock filament were prepared under following conditions for ABS-40% Fe and PA6-40%Fe after conducted pilot experimentations (See Table 3).

Table 3 Input process parameter and their level for screw extrusion

Parameters	ABS-40%Fe	PA6-40%Fe
Temperature (^{o}C)	230	240
Applied Load (Kg)	15	15
Screw speed (rpm)	20	20

It has been observed visually that the dimensional uniformity of feed stock filament/ wire was achieved under these conditions.

2.5FDM (3-D printing)

The finally prepared feedstock filaments were fed to the FDM setup and cylindrical parts were fabricated for friction welding. Fig. 7 shows the FDM setup and fabricated parts of ABS-40%Fe and PA6-40%Fe.

Fig. 7 (a) FDM configuration and (b) Fabricated parts of ABS-40%Fe and PA6-40%Fe

2.6 Friction welding process

The samples/ functional parts were fabricated on FDM (see Fig. 7). The friction welding operation was performed on the center lathe by varying 3 input parameters (namely: rotational speed, feed rate and feed time). The levels of 3 input process parameters were fixed based upon pilot experimentation (to check the feasibility of welding). Fig. 8(a) shows friction welding process (one parts need to be in rotation and other to be fixed). Fig. 8 (b) shows the welded piece of ABS-40%Fe and PA6-40%Fe under 775rpm, 0.09mm/rev and 6 sec. feed time.

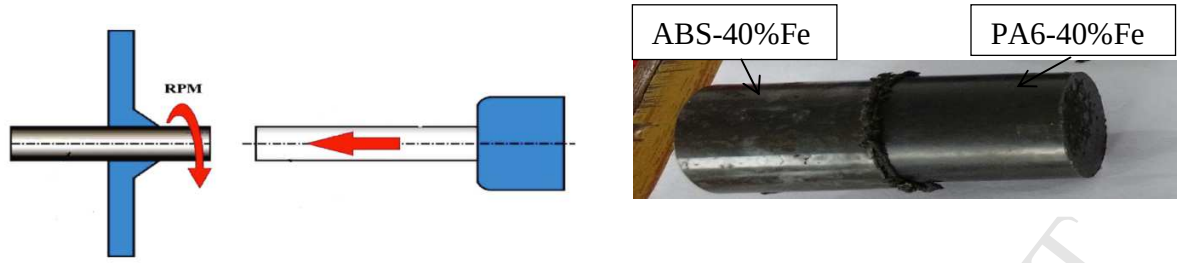

(a) (b)

Fig. 8 (a) Schematic of friction welding process [38] and (b) frictionally welded parts

Based upon pilot experimentation, input process parameters have been selected (See Table 4).

Table 4 Input process parameters and their level

Level	Rotational speed (rpm)	Feed rate (mm/rev)	Feed time(Sec)
1	500	0.045	4
2	775	0.90	6
3	1200	0.18	8

2.7Model developed for mechanical and metallurgical properties

After successful welding operation, different mechanical testing has been performed to investigate the influences of input process parameters. The mechanical and metallurgical properties, namely; Shore D hardness, tensile strength and percentage porosity at joint were checked for each welded samples. Table 5 shows the design of experiment and mechanical and metallurgical properties obtained at specific set of experimental conditions. Total 9 set of experiment have been performed and welded pieces were obtained (See Fig. 9). The optimization was performed with RSM; historical data approach based upon Table 5.

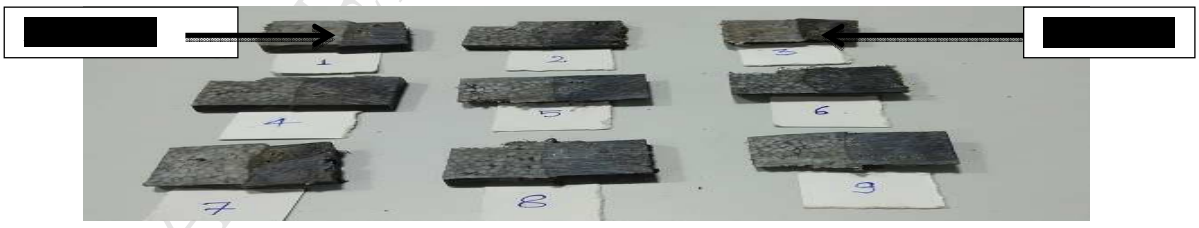

Fig.9 Welded piece (After lateral cutting) under experimentation conditions according to Table 5

Table 5 Input parameter and response parameter for RSM

Run number	Rotational speed (RPM)	Feed rate (mm/rev)	Welding time (Sec)	Shore D hardness (Shore D)	Tensile strength (Kg/mm^2)	Porosity at joint (%)
1	500.00	0.04	4.00	82	0.2351	23.84
2	500.00	0.09	6.00	81.5	0.1898	27.45
3	500.00	0.18	8.00	80.5	0.1601	28.56
4	775.00	0.04	6.00	83	0.2105	24.56
5	775.00	0.09	8.00	82	0.1698	26.56
6	775.00	0.18	4.00	81	0.1324	28.78
7	1200.00	0.04	8.00	82.5	0.2247	22.65
8	1200.00	0.09	4.00	82	0.1786	25.45
9	1200.00	0.18	6.00	81.5	0.1458	27.25

2.7.1 Shore D hardness

It was observed that under these conditions no aliases were found for a linear model. The model were significant as p- value was found lesser than 0.05. Table 6 shows the analysis of variance for shore D hardness, fee rate was considered to be significant as p- value <0.05.

Table 6 analysis of variance table for Shore D hardness

Source	**Sum of squares**	**Degree of freedom**	**Mean square**	**F Value**	**p- value Prob> F**	
Model	3.92	3	1.31	10.31	0.0140	significant
A Rotational Speed	0.57	1	0.57	4.47	0.0883	
B-Feed Rate	3.36	1	3.36	26.47	0.0036	
C-Feed Time	0.000	1	0.000	0.000	1.0000	

The model was under significant residual error as R-squared value obtained greater than 0.8 (See Table 7).

Table 7 Value of R squared

Parameter	**Value**
R-Squared	0.8609
Adjusted R-Squared	0.7774
Predicted R-Squared	0.5790
Adequate Precision	8.785

Now based upon the data obtained from the experimentaton (see Table 5), the following equation can be made for optimization of parameters:

.

Shore D hardness = 82.1484+0.00087Rotational Speed -10.54084FeedRate+0.0Feed Time ……(1)

2.7.1.1 Corrollary (Model Validation)

The model equation (1) was applied by taking ,

Rotational speed -500

Feed rate- 0.045

Feed time- 4 sec

The Shore hardness was obtained 81.7714 as per model equation was closer to the value 82.0 obtained as for these experimental conditions.

2.7.2 Tensile strength

Table 8 shows that model was significant for tensile strength. Feed rate contribute mostly for the changes in tensile strength.

Table 8 analysis of variance for tensile strength

Source	Sum of squares	Degree of freedom	Mean square	F Value	p- value Prob> F	
Model	0.008640	3	0.002880	11.33	0.0114	significant
A-Rotational Speed	0.000129	1	0.000130	0.51	0.5068	
B-Feed Rate	0.008500	1	0.008504	33.42	0.0022	
C-Feed Time	0.000010	1	0.000012	0.047	0.8364	

The model was significant a R-squared value obtained greater than 0.8 (See Table 9)

Table 9 Value of R squared

Parameter	Value
R-Squared	0.8717
Adjusted R-Squared	0.7947
Predicted R-Squared	0.5139
Adequate Precision	7.721

Based upon the result obtained for tensile strength, the model can be express in the form of equation (2)

Tensile strength=0.24445-0.00001319Speed-0.53064FeedRate+0.000708FeedTime ……(2)

2.7.2.1 Corrollary (Model Validation)
The model equation (2) was applied by taking ,
Rotational speed -500
Feed rate- 0.045
Feed time- 4 sec
The tensile strength was obtained 0.2212Kg/mm^{2}as per model equation which was closer to the value obtained as for those experimental conditions 0.2351Kg/mm^2.

2.7.3Percentage porosity at joint

The model was considered to be significant as p value was 0.0086 and feed rate contributed mostly for change over percentage porosity at joint. Table 7 shows the analysis of variance table for percentage porosity.

Table 10 Analysis of variance for percentage porosity at joint

Source	Sum of squares	Degree of freedom	Mean square	F Value	p- value Prob> F	
Model	32.23	3	10.74	12.92	0.0086	significant
A-Rotational Speed	3.83	1	3.83	4.60	0.0848	
B-Feed Rate	28.39	1	28.39	34.13	0.0021	
C-Feed Time	0.015	1	0.015	0.018	0.8984	

R-squared value was obtained greater than 0.8. So model is considered to have significant residual error

Table 11 Value of R squared for percentage porosity

Parameter	Value
R-Squared	0.8857
Adjusted R-Squared	0.8171
Predicted R-Squared	0.5599
Adequate Precision	9.667

Percentage Porosity at joint = +24.97236-0.00226Rotational Speed +30.66004Feed Rate

-0.025000Feed Time …….. (3)

Corrollary (Model Validation)

The model equation (3) was applied by taking ,
Rotational speed -500
Feed rate- 0.045
Feed time- 4 sec
The percentage porosity at was obtained 26.22% as per model equation which was closer to the value obtained as for those experimental conditions 23.84%.

4 Result and discussion

As model obtained are significant with feed rate for all properties like; tensile strength, shore D hardness and percentage porosity at joint. Data obtained from tensile testing were processed through design-expert software to check the characteristics of output parameters in terms of actual value, predicted value, residual, leverage, internally studentized residual, externally studentized residual and cooks distance.

4.1 Shore D hardness

The predictedvalues obtained for shore D hardness at different experimental set up were helpful to calculate the residual of the process. Residual values were further helpful for the calculations of other values like; leverage, studentized residual and cooks distance. Table 12 shows the processed data by design expert software.

Table 12 Data on analysed model for Shore D hardness

Run order	Actual value	Predicted value	Residual	Leverage	Internally studentized residual	Externally studentized residual	Cooks distance
1	82.00	82.16	-0.16	0.552	-0.681	-0.640	0.143
2	81.50	81.64	-0.14	0.259	-0.441	-0.402	0.017
3	80.50	80.69	-0.19	0.614	-0.843	-0.814	0.283
4	83.00	82.40	0.60	0.247	1.936	3.464	0.308
5	82.00	81.87	0.13	0.287	0.417	0.379	0.017
6	81.00	80.93	0.074	0.476	0.287	0.259	0.019
7	82.50	82.77	-0.27	0.599	-1.206	-1.282	0.544
8	82.00	82.24	-0.24	0.472	-0.947	-0.935	0.200
9	81.50	81.30	0.20	0.494	0.804	0.771	0.158

As shown in Fig. 10, there is approximately 50 percentage probability that internally studentized residual will lie near zero. Most of the remaining residuals lies between -1.21 to 0.37.

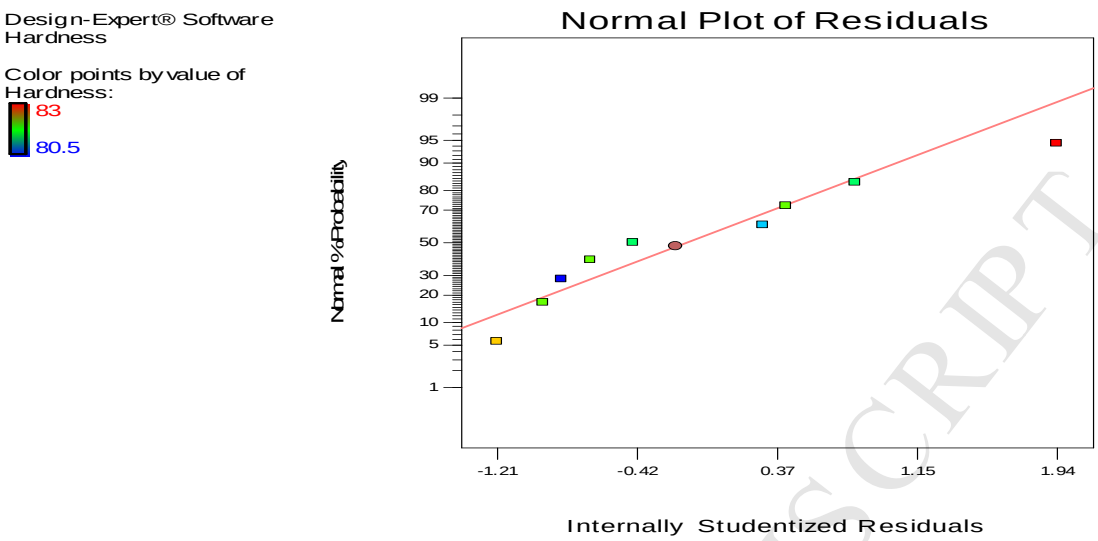

Fig. 10 Normal plot of residuals for shore D hardness

Fig. 11 shows the plot of residual vs. predicted values for shore D hardness. All the points are randomly scattered between red lines, so that measurable of constant variance in data obtained.

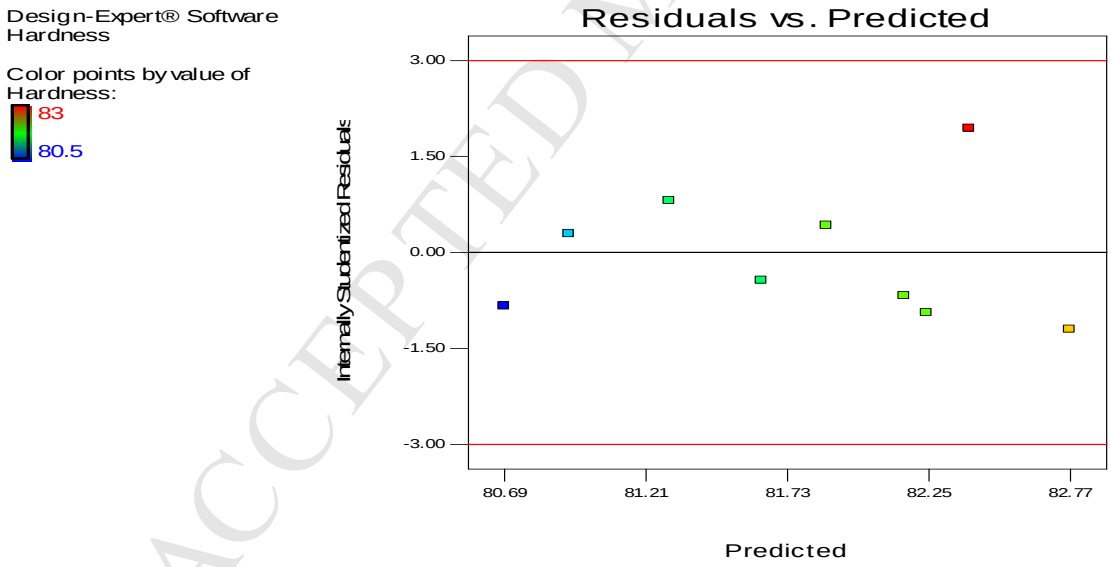

Fig. 11 Plot for residuals vs. predicted value of hardness

A graph has been plotted between predicted values of shore D hardness vs.actual values. The graph show that predicted values are almost coincides with actual values, which confirmed that model was accurate (See Fig. 12).

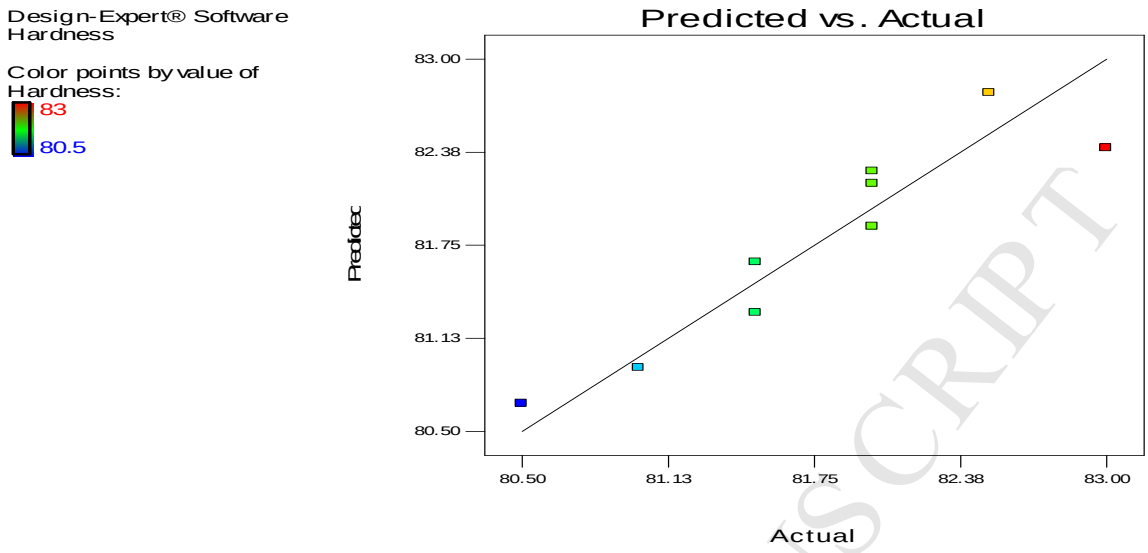

Fig. 12 Plot for predicted vs. actual value for shore D hardness

Another plot has been generated for the cooks distance vs. run number of given output of shore D hardness. All value came under the red line;it confirmed that output of shore D hardness was accurate at given experimental conditions (See Fig. 13).

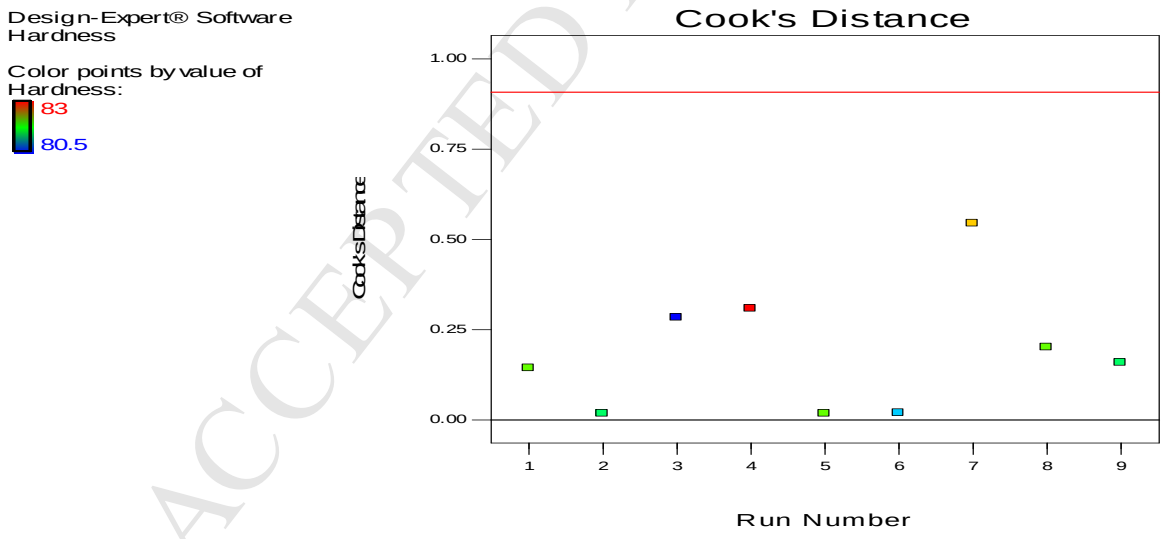

Fig. 13 Plot for cooks distance for shore D hardness

As observed from plot of leverage vs. run, all points scattered below red line. The model confirmed as accurate for given output of shore D hardness at given experimental conditions (See Fig. 14).

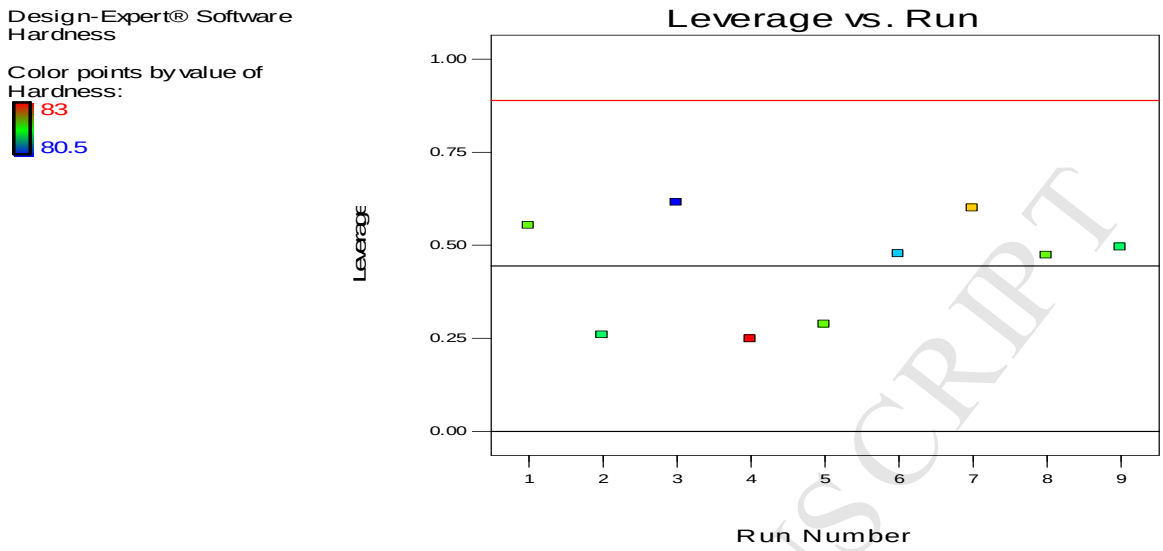

Fig. 14 Plot for Leverage vs. Run for shore D hardness

4.2Tensile strength

As data output data for tensile strength fed to design expert software, Table 13 has been obtained for actual value with which predicted value, residual, leverage, externally studentized residual, externally studentized residual and cooks distance varies.

Table 13 Data on analysed model for tensile strength

Run order	Actual value	Predicted value	Residual	Leverage	Internally studentized residual	Externally studentized residual	Cooks distance
1	0.24	0.22	0.011	0.552	1.465	1.735	0.662
2	0.19	0.19	-0.004	0.259	-0.331	-0.299	0.010
3	0.16	0.15	0.006	0.614	1.221	1.303	0.592
4	0.21	0.22	-0.006	0.247	-0.487	-0.447	0.020
5	0.17	0.19	-0.022	0.287	-1.658	-2.209	0.277
6	0.13	0.14	-0.009	0.476	-0.791	-0.757	0.142
7	0.22	0.21	0.012	0.599	1.153	1.204	0.497
8	0.18	0.18	-0.005	0.472	-0.439	-0.400	0.043
9	0.15	0.14	-0.008	0.494	0.745	0.707	0.136

A graph has been plotted for normal probability against internally studentized residual as shown in Fig. 15. Most of the values of residual lay around red line, so model is determined as significant.

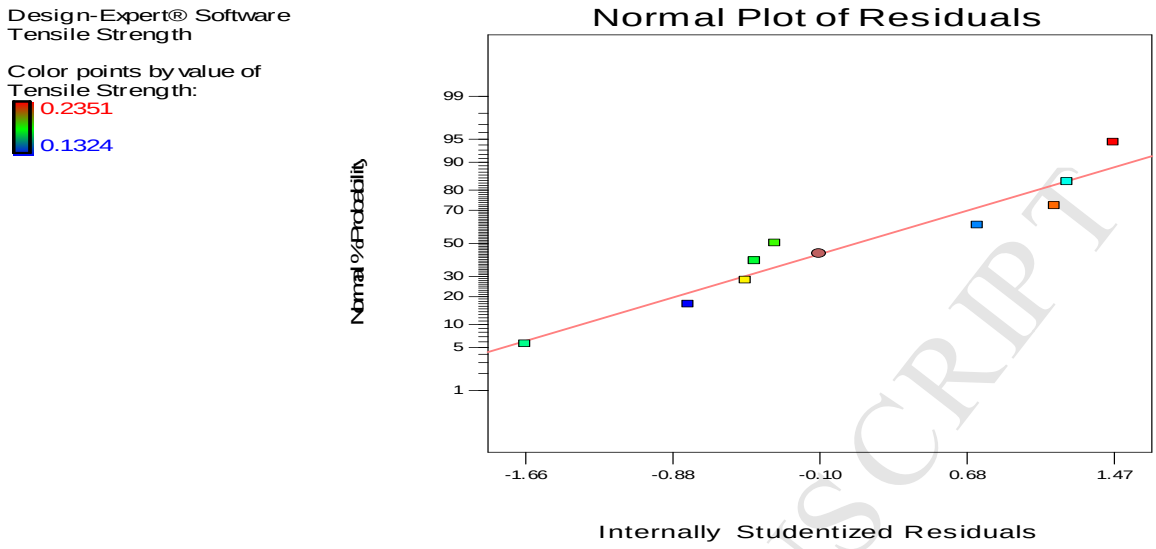

All 9 predicted values of tensile strength lies between red lines, so predicted value are assumed to be accurate with given experimental conditions (See Fig. 15).

Fig. 15 Normal plot of residuals for tensile strength

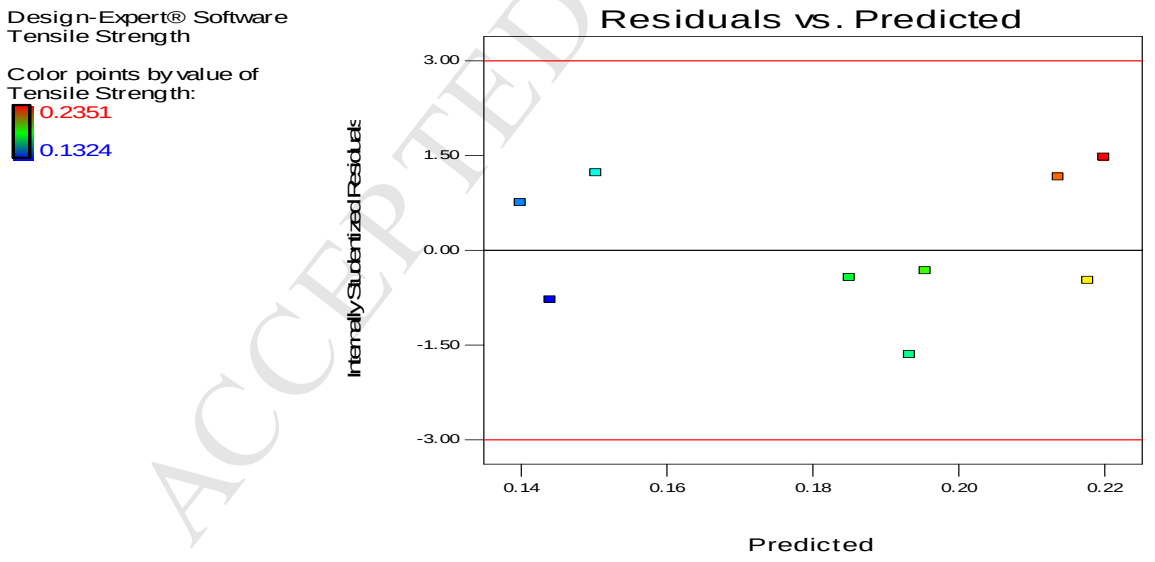

Fig. 16 Plot for residuals vs. predicted value of tensile strength

As actual values are coinciding to the red line, it confirmed that model is accurate for tensile strength of given values (See Fig. 17).

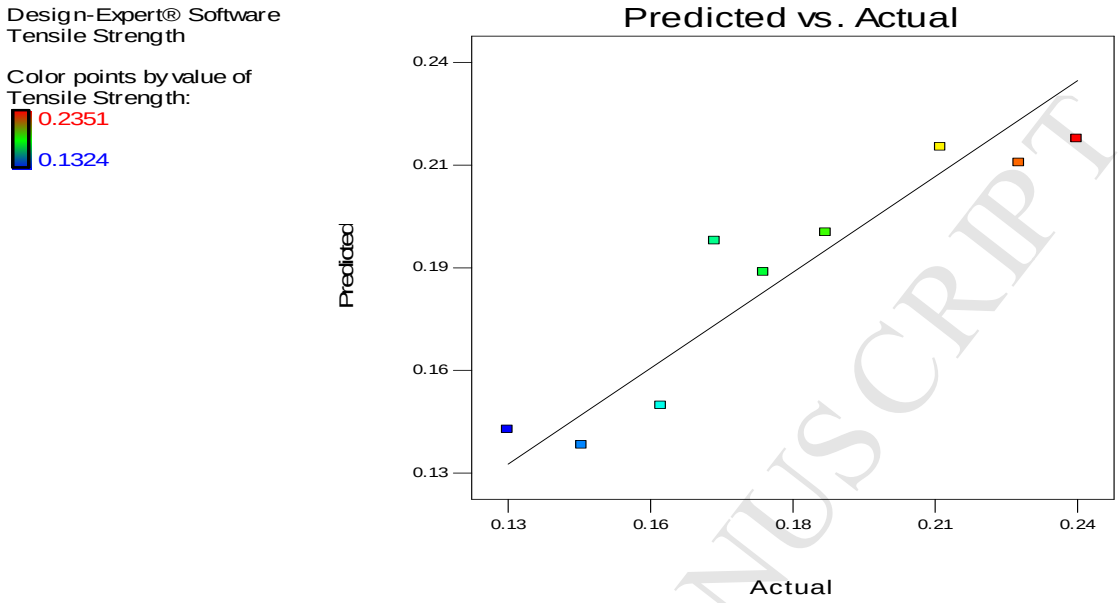

Fig. 17 Plot for predicted vs. actual value for tensile strength

As shown in Fig. 18 and Fig. 19, cooks distance and leverage have been plotted against run number. All the values are come under red line considered that model was significant under those experimental conditions.

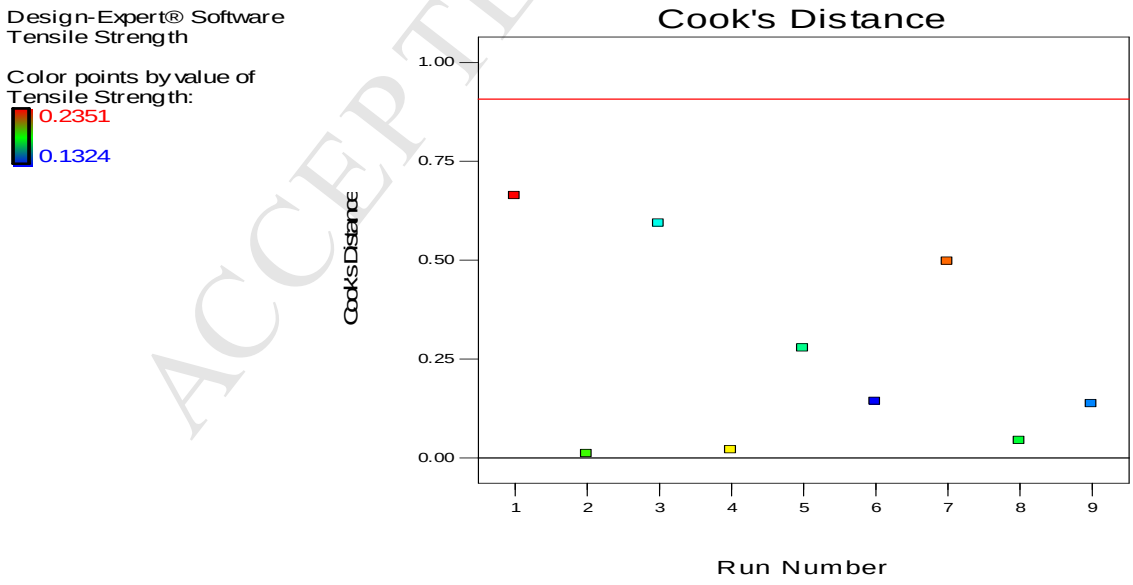

Fig. 18 Plot for cooks distance for tensile strength

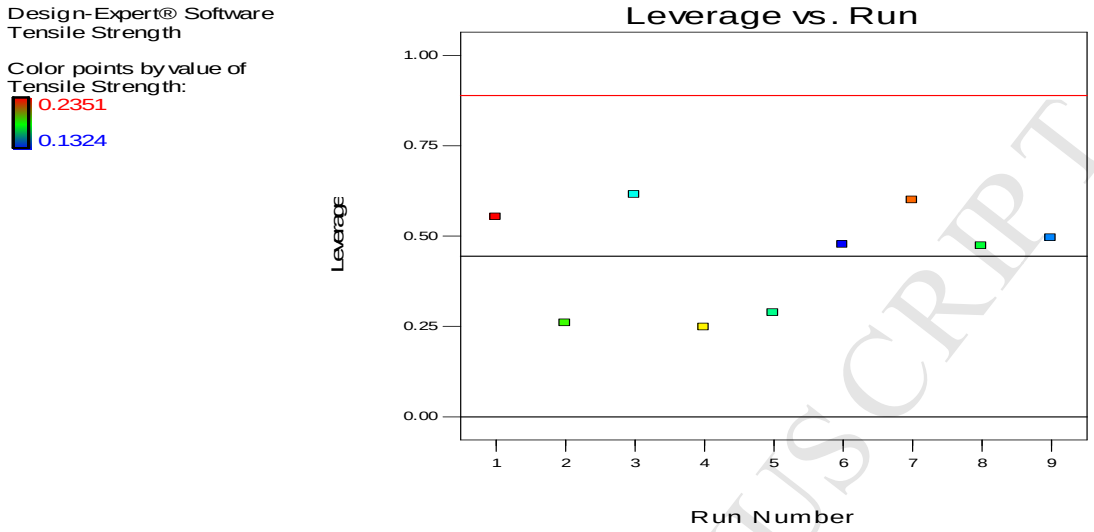

Fig. 19 Plot for Leverage vs. Run for tensile strength

4.3Percentage porosity at joint

Table 14 has been obtained for actual values of percentage porosity at joint vs. predicted values and residual.

Table 14 Data on analyzed model for percentage porosity at joint.

Run order	Actual value	Predicted value	Residual	Leverage	Internally studentized residual	Externally studentized residual	Cooks distance
1	23.84	24.97	-1.13	0.552	-1.846	-2.924	0.105
2	27.45	26.45	1.00	0.259	1.274	1.387	0.142
3	28.56	29.16	-0.60	0.614	-1.057	-1.073	0.444
4	24.56	24.29	0.27	0.247	0.337	0.305	0.009
5	26.56	25.78	0.78	0.287	1.017	1.022	0.104
6	28.78	28.64	0.14	0.476	0.218	0.196	0.011
7	22.65	23.28	-0.63	0.599	-1.093	-1.121	0.446
8	25.45	24.91	0.54	0.472	0.809	0.776	0.146
9	27.25	27.62	-0.37	0.494	-0.576	-0.533	0.081

Fig. 20 shows the normal plot of residual for percentage porosity obtained. Internally studentized residual values are almost near about red line, so it can be determined as model was accurate and significant for given output.

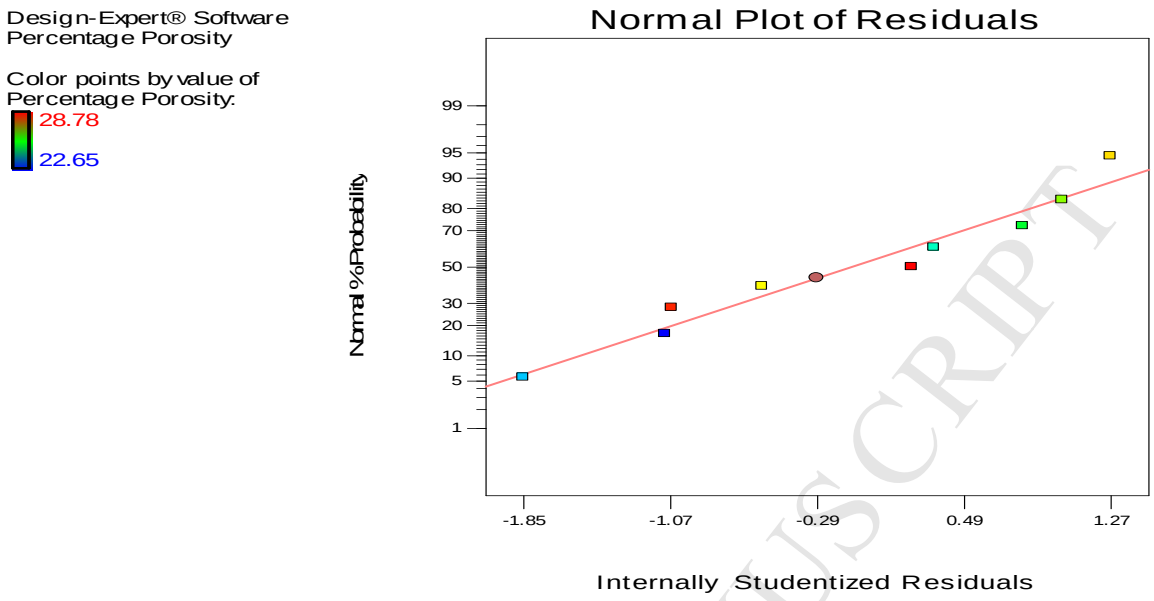

Fig. 20 Normal plot of residuals for percentage porosity

The predicted values lie under red lines, so model can be assumed as significant for given output range (See Fig. 21).

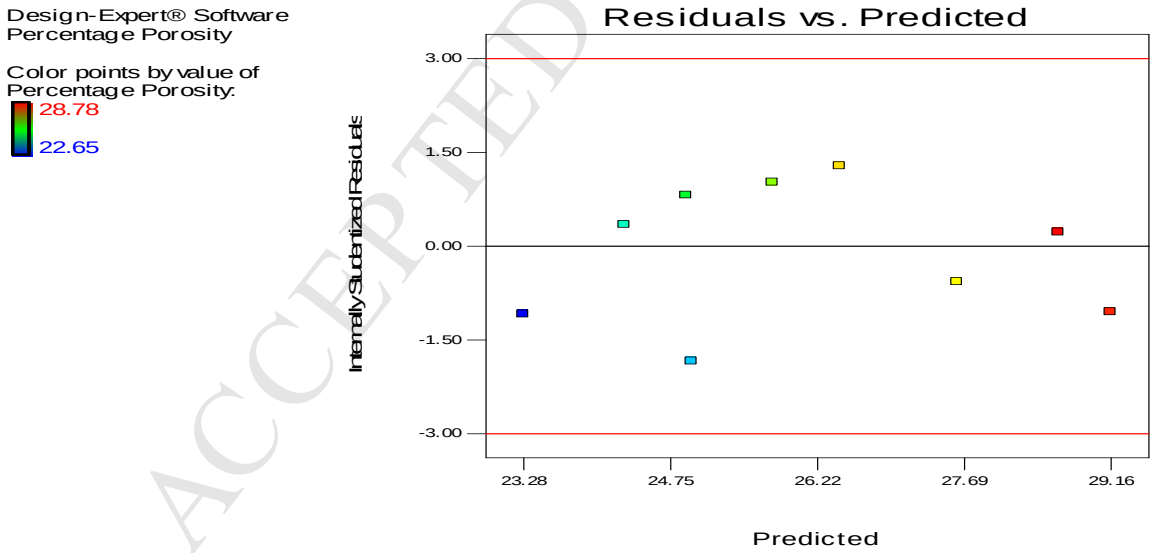

Fig. 21 Plot for residuals vs. predicted value of percentage porosity

A plot has been generated for the predicted values of porosity vs. actual value as shown in Fig. 22. The values are lying around the straight line, it can be considered as model was significant with desirable accuracy

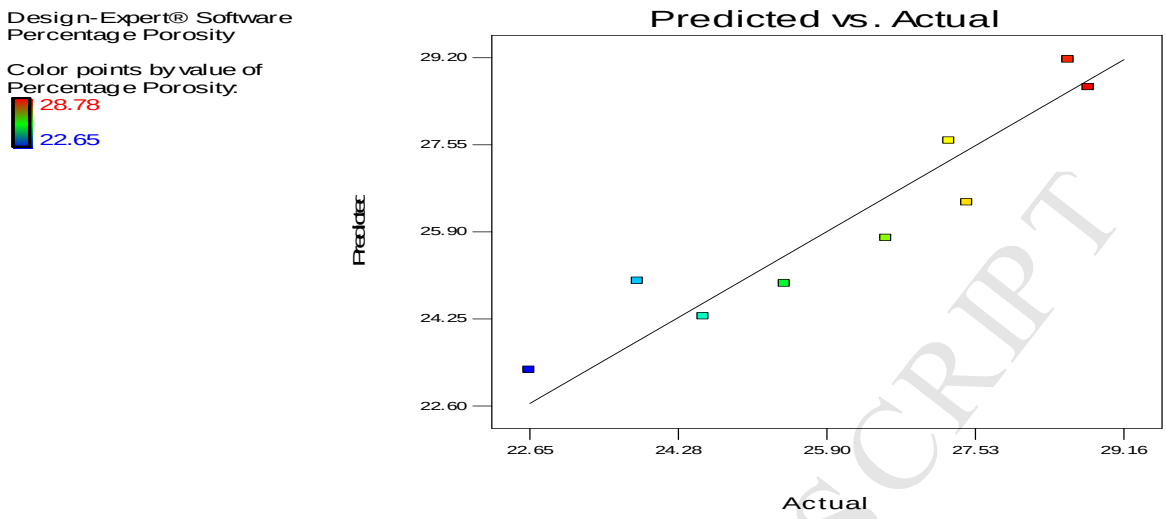

Fig. 22 Plot for predicted vs. actual value for percentage porosity

Fig. 23 shows the plot of cooks distance vs. run number for given output of percentage porosity at joint. Except one value other 8 values of porosity was come under red line. So it was measurable that model of experimental setup was almost significant.

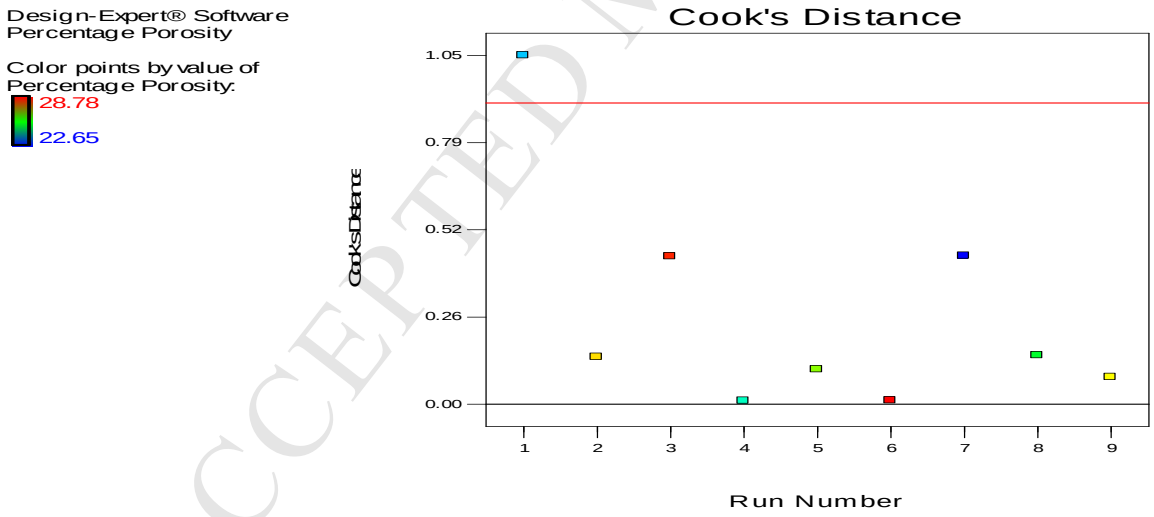

Fig. 23 Plot for Leverage vs. Run for percentage porosity

Fig. 24 shows the leverage vs. run number for given output of percentage porosity. All the values of percentage porosity lie under red line, so that model was assumed to be accurate and acceptable.

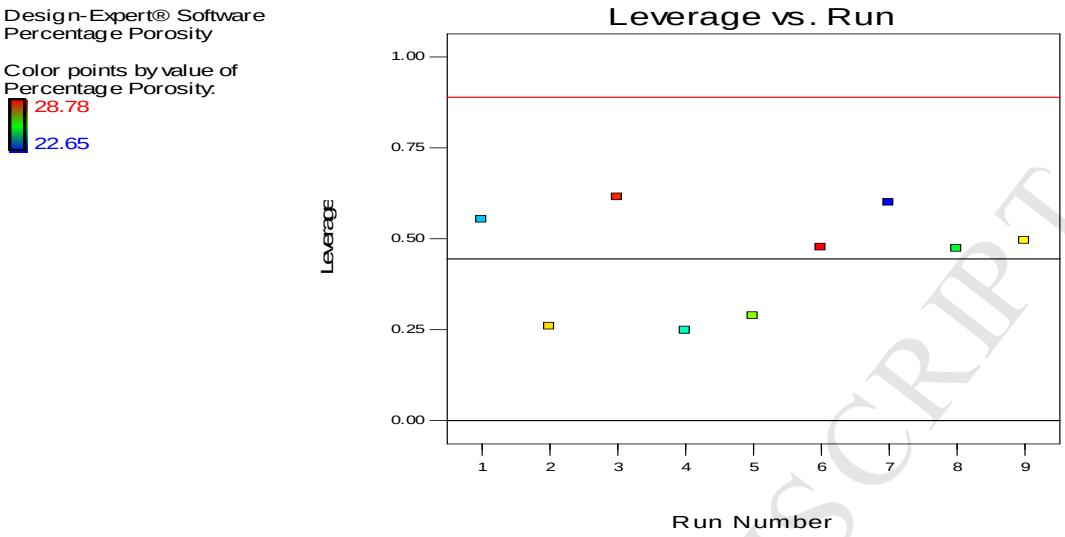

Fig. 24 Plot for cooks distance for percentage porosity

5. Conclusions

Initial experimentation of rheology and DSC has been performed for compatibility analysis of ABS and PA6 polymer matrix whereas mechanical properties were investigated for joining characteristics of Fe reinforced ABS and PA6 polymer matrix. Following conclusions can be made from the present research work:-

- ABS and PA6 polymer matrix at 40% Fe powder contributed to similar rheological property. Similar rheological property achieved by Fe metal powder reinforcement has further resulted in similar melting behavior.
- Welding of natural ABS with natural PA6 was unsuccessful. But Fe metal powder at certain concentration led to similar rheological and melting properties offered successful welding of ABS and PA6.
- Model developed for output properties like; Shore D hardness, tensile strength and percentage porosity was significant. Feed rate has been considered as most significant input parameters for said outputs. The experiment no. 7 (as per Table 5) has resulted in better mechanical and metallurgical properties, which has high rpm, low feed rate and high feed time configurations.

Future work will address the employment of micromechanics and poroelasticity [47]-[48] for the mechanical modeling of the analyzed materials, as well as the use of plastic waste [49] for the fabrication of composite materials and structures that are made out of such materials [50]-[63].

Acknowledgements

The authors are highly thankful to Board of research in nuclear science (BRNS) and University grant commission (UGC) for providing financial assistance to carry out the research work.

References:

[1] Givi M. K. B. and Asadi P. (1981), “Advances in Friction Stir welding and processing”,*General introduction* pp1-19.DOI: 10.1533/9780857094551.1

[2] Rashid H. , Hunt K. N. & Evans J. R. G. (1991) “Joining ceramics before firing by ultrasonic welding”, *Journal of the European Ceramic Society* vol. 8pp329-338

[3] Kathirgamanathan P. (1993) “Microwave welding of thermoplastics using inherently conducting polymers”. *Journal of polymer communications*. vol. 34 pp3105-3106

[4] Shim M.-J., Kim S.-W., (1997) "Characteristics of polymer welding by healing process",*Journal of materials chemistry and physics*. Vol. 48. pp90-93

[5] Brown N., Kerr D., Jackson M.R., Parkin R.M. (2000) "Laser welding of thin polymer film to container substrate for aseptic packaging", *Journal of Optics & Laser Technology*. vol. 32. pp139-146

[6] Haire K.R., Windle A.H. (2001) "Monte Carlo simulation of polymer welding", *journal computational and theoretical polymer science*. vol. 11 pp227-240

[7] Stokes V. K. (2001)"A phenomenological study of the hot-tool welding of thermoplastics Part 3 Polyetherimide", Journal of polymer. Vol. 42, pp775-792.

[8] Anderson K.L., Wescott J.T., Carver T.J., Windle A.H. (2004) "Mesoscale modelling of polymer welding". *Jornal of material science and engineering* A. vol. 365, pp14-24

[9] Bates P.J., Mah J.C., Zou X.P., Wang C.Y., Baylis Bobbye., (2004)"Vibration welding air intake manifolds from reinforced nylon 66, nylon 6 and polypropylene". *Journal of Composite Part A: applied science and manufacturing*. vol. 35, pp 1107-1116.

[10] Stavrov D., Bersee H.E.N. (2005) "Resistance welding of thermoplastic composites- an overview*"*. *Journal of Composite Part A: applied science and manufacturing*. vol. 36, pp39-54.

[11] Ageorges C., Ye L. (2001)"Resistance welding of thermosetting composite/thermoplastic composite joints". *Journal of Composite part A: applied science and manufacturing*. vol. 32, pp1603-1612

[12] Xie L, Liu H. Wu W.,Abliz D., Duan Y., Li D., (2016) "Fusion bonding of thermosets composite structures with thermoplastic binder co-cure and prepreg interlayer in electrical resistance welding" *Journal of Materials and Design*. vol. 98, pp143-149

[13] Awaja F. (2016) "Autohesion of polymers". Journal of polymers. vol. 97. pp387-407

[14] Taylor NS, Jones SB, Weld M. (1989)”The feasibility of welding thermoplastic composite materials”. *Construction Building Materials*. Vol. 3, 213–219.

[15] Yilbas B. S., Şahin A.Z., Kahramanb N., Al-Garni A. Z.,(1995)"Friction welding of St-Al and Al-Cu materials". Journal of MaterialProcessing Technology. Vol. 49, pp431-443

[16] Kostka A., Coelho R.S., Santos J.D., Pyzalla A.R., (2009)"Microstructure of friction stir welding of aluminium alloy to magnesium alloy", *Journal of Scripta Materialia*. Vol. 60, pp953–956

[17] Gao J., Li C., Shilpakar U., Shen Y., (2015)"Improvements of mechanical properties in dissimilar joints of HDPE and ABS via carbon nanotubes during friction stir welding process",*Material Design*. Vol. 86, pp289-296

[18] Sluzalec A., (1990)"Thermal effects in friction welding", *International Journal of Mechanical Sciences.* Vol. 32, pp467–478

[19] Stokes V.K., Hobbs S.Y.,(1993)"Vibration welding of ABS to itself and to polycarbonate, poly(butylene terephthalate), poly(ether imide) and modified poly(phenylene oxide)",*Jornal of Polymer*. Vol. 34(6): pp1222-1231

[20] Stokes V.K., (1993)"The effect of fillers on the vibration welding of poly(butylene Terephthalate)". Journal of Polymer; vol 34(21):pp4445-4454

[21] Yılmaz M., Col M., Acet M. (2002), "Interface properties of aluminum/steel friction welded components". *Mater Charact*;49(5):421-429.

[22] Rotundo F, Ceschini L, Morri A, Jun TS, Korsunsky AM. (2010) "Mechanical and microstructural characterization of 2124Al/25 vol.%SiCp joints obtained by linear friction welding' (LFW). *Compos Part A-Appl S*;41(9):1028–1037.

[23] Panneerselvam K, Lenin K. (2014), "Joining of Nylon 6 plate by friction stir welding process using threaded pin profile",Mater Design;53:302-307.

[24] Faes K, Dhooge A, Baets PD, Donckt EV, Waele WD. (2009) "Parameter optimisation for automatic pipeline girth welding using a new friction welding method",*Mater Design*;30(3):581–589.

[25] Attallah MM. (2012) "Inertia friction welding (IFW) for aerospace applications. In Welding and Joining of Aerospace Materials", M Chaturvedi(Ed.), *Woodhead Publishing*, 25–74,.

[26] Raab U, Levina S, Wagnera L, Heinze C. (2015)"Orbital friction welding as an alternative process for blisk manufacturing",*J Mater Process Tech*;215(1):189-192.

[27] Junior WS, Handge UA, Jorge F, Abetz V, Filho STA. Feasibility study of friction spot welding of dissimilar singlelap joint between poly(methyl methacrylate) and poly(methyl methacrylate)SiO2 nanocomposite. *Mater Design* 2014;215:246-250.

[28] D'Alvise L, Massoni E, Walloe SJ. Finite element modelling of the inertia friction welding process between dissimilar materials. *J Mater Process Tech* 2002;125-126(9):387-391.

[29] Healy JJ, McMullan DJ, Bahrani AS. Analysis of frictional phenomena in friction welding of mild steel. *Wear* 1976;37(2):265–278.

[30] Hoseinlaghab, S., Mirjavadi, S.S., BesharatiGivi, M.K., Azarbarmas, M., Influences of welding parameters on the quality and creep properties of friction stir welded

polyethylene plates, *Materials and Design* (2014), doi: http://dx.doi.org/10.1016/j.matdes.2014.11.039

[31] Inaniwa S, Kurabe Y, Miyashita Y, Hori H. Application of friction stir welding for several plastic materials. In: Proceedings of the 1st International Joint Symposium on Joining and Welding Osaka 2013, Japan 2013;137-142.

[32] Ji Y, Chai Z, Zhao D, Wu S. Linear friction welding of Ti–5Al–2Sn–2Zr–4Mo–4Cr alloy with dissimilar microstructure. *J Mater Process Tech* 2014;214(4):979-987

[33] Fu, S-Y. and Lauke, B., (1998), "Characterization of tensile behaviour of hybrid short glass fibre/calcite particle/ABS composites", *Composite Part A*, Vol. 29, No. 1, pp. 575-583.

[34] Kang, T-K., Kim, Y., Cho, W-J.and Ha, C-S. (1997), "Effects of Amorphous Nylon on the Properties of Nylon 6", *polymer Testing*, Vol. 1, No. 1, pp. 391-401.

[35] Kudva, R.A., Keskkula, H. and Paul, D.R. (1998), "Compatibilization of nylon 6/ABS blends using glycidyl methacrylate/methyl methacrylate copolymers", *Polymer*, Vol. 39, No. 12, pp. 2447-2460.

[36] Hale, W., Lee, J-H., Keskkula, H. and paul, D.R. (1999), "Effect of PBT melt viscosity on the morphology and mechanical properties of compatibilized and uncompatibilized blends with ABS", *Polymer*, Vol. 40, No. 1, pp. 3621-3629.

[37] Harris, F.W., Livengood, B.P., Ding, H., Lin, F.L. and Cheng, S.Z.D. (1996), "Mechanical reinforcement and thermal transition behaviors in nylon 6-b-polyimide-b-nylon 6 triblock copolymers", *ThermochimicaActa*, Vol. 272, No. 1, pp. 157-169.

[38] E. P. Alves, F. P. Neto& C. Y. An, "Welding of AA1050 aluminum with AISI 304 stainless steel by rotary friction welding process", Aerospace technology management , Vol. 2, 2010, pp. 301-306.

[39] Singh, R., Kumar, R., Feo, L. and Fraternali, F. (2016) "Friction welding of dissimilar plastic/polymer materials with metal powder reinforcement for engineering applications", *Composites Part B*, Vol. 101, No. 1, pp. 77-86.

[40] Ferg, E.E. and Bolo, L.L.,. A correlation between the variable melt flow index and the molecular mass distribution of virgin and recycled polypropylene used in the manufacturing of battery cases. *Polymer Testing* 2013; 32(8): 1452–1459.

[41] Bremner, T., Rudin,A., and Cook,D.G. (1990), "Melt flow index values and molecular weight distributions of commercial thermoplastics", *J. Appl. Pol. Sci.*, Vol. 41, No.7–8, pp.1617–1627

[42] Dutta,A. (1984), "'On viscosity – melt flow index relationship", *RheologicaActa*, Vol. 23 , No. 5, pp. 565–569.

[43] Nichetti, A D. and I. Manas-Zloczower, Viscosity model for polydispersepolymermelts. J. *Rheology*1998; 42(4):951–969.

[44] Shenoy, A.V., Chattopadhyay,S., and Nadkarni, V.M. (1983), "From melt flow index to rheogram", *RheologicaActa*, Vol. 22, No. 1, pp. 90–101.

[45] Teresa Rodríguez-Hernández, M., Angulo-Sánchez, J.L. and. Pérez- Chantaco, A. (2007), "Determination of the molecular characteristics of commercial polyethylenes with different architectures and the relation with the melt flow index", *J. Appl. Pol. Sci*, Vol. 104, No. 3, pp.1572–1578.

[46] ZulkifliMohamadAriff A.A., Jikan, S. S.,and Abdul Rahim, N. A. (2012), "Rheological Behaviour of Polypropylene Through Extrusion and Capillary Rheometry, Polypropylene in Polypropylene", (Ed) D.F. Dogan, InTech Open Science Croatia

[47] A. Lucantonio, G. Tomassetti, A. De Simone, Large-strain poroelastic plate theory for polymer gels with application to swelling-induced morphing of composite plates. Composites Part B: Engineering, 115, 330-340, 2017.

[48] H. Khezrzadeh, A statistical micromechanical multiscale method for determination of the mechanical properties of composites with periodic microstructure. Composites Part B: Engineering, 115, 138-143, 2017.

[49] N. Singh, D. Hui, R. Singh, I.P.S. Ahuja, L. Feo, F. Fraternali, Recycling of plastic solid waste: A state of art review and future applications. Composites Part B: Engineering, 115, 409-422, 2017.

[50] F. Naddeo, A. Naddeo, N. Cappetti, Novel "load adaptive algorithm based" procedure for 3D printing of lattice-based components showing parametric curved micro-beams. Composites Part B: Engineering, 115, 51-59, 2017.

[51] F. Fraternali, S. Spadea, V.P. Berardi, Effects of recycled PET fibers on the mechanical properties and seawater curing of Portland cement-based concretes. Construction and Building Materials, 61, 293-302, 2014.

[52] S. Spadea, I. Farina, A. Carrafiello, F. Fraternali, Recycled nylon fibers as cement mortar reinforcement Construction and Building Materials, 80, 200-209, 2015.

[53] I. Farina, F. Fabbrocino, G. Carpentieri, M. Modano, A. Amendola, R. Goodall, L. Feo, F. Fraternali, On the reinforcement of cement mortars through 3D printed polymeric and metallic fibers, Composites Part B: Engineering, 90, 76-85, 2016.

[54] Farina, I., Fabbrocino, F., Colangelo, F., Feo, L., Fraternali, F., Surface roughness effects on the reinforcement of cement mortars through 3D printed metallic fibers. Composites Part B: Engineering, 99, 305-311, 2016.

[55] F. Naddeo, A. Naddeo, N. Cappetti, Novel "load adaptive algorithm based" procedure for 3D printing of cancellous bone-inspired structures. Composites Part B: Engineering, 115, 60-69, 2017.

[56] R. Singh, R. Singh, J.S. Dureja, I. Farina, F. Fabbrocino, Investigations for dimensional accuracy of Al alloy/Al-MMC developed by combining stir casting and ABS replica based investment casting. Composites Part B: Engineering, 115, 203-208, 2017.

[57] A. Amendola, E.H. Nava, R. Goodall, I. Todd, R.E. Skelton, F. Fraternali, On the additive manufacturing, post-tensioning and testing of bi-material tensegrity structures, Composite Structures, 131, 66-71, 2015.

[58] A. Amendola, G. Carpentieri, M. de Oliveira, R.E. Skelton, F. Fraternali, Experimental investigation of the softening stiffening response of tensegrity prisms under compressive loading. Composite Structures, 117, 234-243, 2014.

[59] D. Ngo, F. Fraternali, C. Daraio, Highly Nonlinear Solitary Wave Propagation in Y-Shaped Granular Crystals with Variable Branch Angles. Physical Review E, 85, 036602-1-10, 2012.

[60] F. Fraternali, A. Marino, T. Elsayed, A. Della Cioppa, On the structural shape optimization via variational methods and evolutionary algorithms. Mechanics of Advanced Materials and Structures, 18, 225-243, 2011.

[61] Fraternali, F., Amendola, A. Mechanical modeling of innovative metamaterials alternating pentamode lattices and confinement plates. Journal of the Mechanics and Physics of Solids, 99, 259-271, 2017.

[62] Amendola, A., Benzoni, G., Fraternali, F. Non-linear elastic response of layered structures, alternating pentamode lattices and confinement plates. Composites Part B: Engineering, 115, 117-123, 2017.

[63] A. Amendola, C.J. Smith, R. Goodall, F. Auricchio, L. Feo, G. Benzoni, F. Fraternali, Experimental response of additively manufactured metallic pentamode materials confined between stiffening plates. Composite Structures, 142, 254-262, 2016.